HAL
open science

Last Glacial Maximum active layer thickness in Western Europe, and the issue of 'tundra gleys' in loess sequences

Pascal Bertran, Kim Stadelmaier, Patrick Ludwig

To cite this version:

Pascal Bertran, Kim Stadelmaier, Patrick Ludwig. Last Glacial Maximum active layer thickness in Western Europe, and the issue of 'tundra gleys' in loess sequences. Journal of Quaternary Science, 2022, 10.1002/jqs.3434 . hal-03691433

HAL Id: hal-03691433

https://hal.science/hal-03691433v1

Submitted on 9 Jun 2022

HAL is a multi-disciplinary open access archive for the deposit and dissemination of scientific research documents, whether they are published or not. The documents may come from teaching and research institutions in France or abroad, or from public or private research centers.

L'archive ouverte pluridisciplinaire **HAL**, est destinée au dépôt et à la diffusion de documents scientifiques de niveau recherche, publiés ou non, émanant des établissements d'enseignement et de recherche français ou étrangers, des laboratoires publics ou privés.

JOURNAL OF QUATERNARY SCIENCE (2022) 1–7 ISSN 0267-8179. DOI: 10.1002/jqs.3434

JQS Journal of Quaternary Science QRA Quaternary Research Association

Last Glacial Maximum active layer thickness in Western Europe, and the issue of 'tundra gleys' in loess sequences

PASCAL BERTRAN,[1,2]* KIM H. STADELMAIER[3] and PATRICK LUDWIG[3]
[1]Inrap, 140 avenue du Maréchal Leclerc, 33130, Bègles, France
[2]PACEA, UMR 5199, Université de Bordeaux-CNRS, bâtiment B2, allée Geoffroy-Saint-Hilaire, 33605, Pessac, France
[3]Institute of Meteorology and Climate Research, Karlsruhe Institute of Technology, Karlsruhe, Germany

Received 24 February 2022; Revised 11 April 2022; Accepted 26 April 2022

ABSTRACT: Late Marine Isotope Stage (MIS) 3 and MIS 2 loess–palaeosol sequences in Western Europe comprise alternating loess layer and 3- to 30-cm-thick bleached soil horizons with Fe–Mn oxide precipitations, which are usually interpreted as waterlogged active layers and referred to as 'tundra gleys'. Active layer thickness data derived from a regional climate model simulation and the fossils (shells, earthworm granules) found in 'tundra gleys' argue against such an assumption. Most of these horizons better correspond to Fe-depleted, slightly humic topsoil horizons or subsurface eluvial horizons and should be referred to as (incipient) Ag or Eg horizons. They formed during climate ameliorations associated with vegetation (cryptogams, herbs) development, possibly limited by long-lasting snow cover. Strong mixing usually occurred in these horizons due to the activity of anecic earthworms and frost activity.
© 2022 The Authors. *Journal of Quaternary Science* Published by John Wiley & Sons Ltd.

KEYWORDS: active layer thickness; loess–palaeosol sequences; permafrost; regional climate modelling; tundra gley; Western Europe

Introduction

In recent decades, much effort has been devoted to reconstructing the extent of Last Glacial Maximum (LGM) permafrost in Europe using field evidence and palaeoclimate simulations (e.g. Levavasseur *et al.*, 2011; Vandenberghe *et al.*, 2014; Kitover *et al.*, 2016; Andrieux *et al.*, 2016; Stadelmaier *et al.*, 2021; Bertran, 2022). While our knowledge of LGM environments has increased substantially as a result of these studies, little attempt has been made to re-evaluate the significance of permafrost-related features in loess–palaeosol sequences (LPS), which are the main source of palaeoenvironmental information on the continent for the Last Glacial. Of particular interest are the bleached horizons often referred to as 'tundra gleys', which were assumed to correspond to waterlogged active layers. Here we try to demonstrate that such an assumption cannot be accepted in most cases based on a series of arguments, mainly data on active layer thickness (ALT) and fossils (shells, earthworm granules) usually found in the palaeosols. As the criteria for assessing ALTs from field data are not straightforward, estimates of ALTs were derived here from a regional climate model simulation that was used for LGM permafrost reconstruction by Stadelmaier *et al.* (2021). The implications of the new interpretation proposed of 'tundra gleys' are then discussed.

Methods

We use a regional climate model simulation conducted with the Weather Research and Forecasting model (WRF Version 4.1.2; Skamarock *et al.*, 2019), and driven by the global MPI-ESM-P simulation for the LGM (Jungclaus *et al.*, 2013; Stevens *et al.*, 2013). The details of the model set-up are described in Stadelmaier *et al.* (2021) as well as the assessment of the mean climate in both global driving and regional simulations. Thirty-two years were dynamically downscaled to a horizontal resolution of 50 km (domain 1) and 12.5 km (domain 2). The first 2 years are excluded from further analysis to ensure a sufficient spin-up time of the model simulation. Land surface and soil characteristics are parametrized with the unified Noah land surface model (Tewari *et al.*, 2004) covering four discrete soil layers with representative depths of 0.05, 0.25, 0.7 and 1.5 m, respectively. In total, a soil column of up to 2 m depth is considered.

The simulated permafrost distribution is derived based on the surface frost index (SFI; Nelson and Outcalt, 1987). This index takes annual freezing and thawing degree-days (DDF and DDT, respectively) into account, which are the sum of daily temperatures below or above 0 °C respectively. Whereas Stadelmaier *et al.* (2021) used the third model layer with a representative depth of 0.7 m to ensure comparability between the global and regional simulations, we here derive the permafrost distribution based on the lowermost soil layer at 1.5 m. As in Stadelmaier *et al.* (2021), the reconstructed permafrost extent is compared with the distribution of ice-wedge pseudomorphs proposed by Isarin *et al.* (1998) for northern Europe and Andrieux *et al.* (2016) for France.

In the permafrost areas thereby identified, we deduce the ALTs with a method after Koven *et al.* (2013). Vertical soil profiles of mean monthly temperatures are generated via linear regressions and with a low weight of the uppermost soil temperature for each model grid cell. The intersection with 0 °C marks the thaw depth for the given month. Considering only thaw depths between 0 and 3 m, the annual ALTs are found as the maximum thaw depths for a given year and are then averaged over 30 years.

*Correspondence: P. Bertran, as above.
E-mail: pascal.bertran@inrap.fr

© 2022 The Authors. *Journal of Quaternary Science* Published by John Wiley & Sons Ltd.
This is an open access article under the terms of the Creative Commons Attribution-NonCommercial-NoDerivs License, which permits use and distribution in any medium, provided the original work is properly cited, the use is non-commercial and no modifications or adaptations are made.

Tundra gleys

In many LPS from Western Europe, the Late Marine Isotope Stage (MIS) 3 and MIS 2 deposits comprise alternating loess layers and bleached soil horizons usually 3–30 cm thick with Fe–Mn oxide precipitates, which are interpreted as 'tundra gleys' or 'micro-tundra gleys' depending on their thickness. This type of horizon was first identified in Belgium and Germany (e.g. Gullentops, 1954, 1981; Rohdenburg and Meyer, 1966). Similar horizons were later found in many European LPS (e.g. Vandenberghe *et al.*, 1998; Vandenberghe and Nugteren, 2001; Antoine *et al.*, 2009; Kadereit *et al.*, 2013; Terhorst *et al.*, 2015; Fischer *et al.*, 2020; Schmidt *et al.*, 2021; Moine *et al.*, 2021) and referred to as 'tundra gleys' by comparison with modern High-Arctic soils (e.g. Tedrow, 1966, 1968; to our knowledge this term was first used by Haesaert and Van Vliet-Lanoë, 1981), 'Gelic Gleysols' according to the FAO (1974) soil classification or 'Cryosol' according to World Reference Base for Soil Resources (IUSS Working Group WRB, 2015). These horizons are usually typified by (i) a greyish colour ranging from pale to dark grey, the latter testifying to slight staining by organic matter, (ii) often a finer-grained texture than the underlying loess material, (iii) slight to complete decalcification, (iv) small Fe–Mn oxide nodules scattered throughout the horizon – Fe oxide-stained fringes around small root channels can be seen in the lower part or below the horizon, and (v) sometimes clear evidence of soil churning due to cryoturbation or solifluction (on slopes) (Fig. 1). Significant variability is obvious. Some bleached horizons appear in isolation in the loess sequence (Fig. 1B), while others overlay a weakly developed brown Bw-like horizon (Fig. 1A) or a cryoturbated C or Cg horizon (Fig. 1C, D). A thin slightly organic grey brown horizon is sometimes visible at the top (Fig. 1A). The idea that all these bleached horizons formed in connection with impeded drainage above permafrost is widely shared among loess scientists. In particular, their occurrence in porous sediments (loess) and in topographic locations (i.e. upslope) a priori unfavourable to waterlogging was considered a decisive argument (e.g. Gullentops, 1981; Terhorst *et al.*, 2015).

Recently, detailed analysis of the assemblages of molluscan shells associated with 'tundra gleys' has provided evidence for temperature improvement during their formation (Moine *et al.*, 2008, 2021). Radiocarbon dating of shells and calcitic earthworm granules also convincingly places their development within interstadials (Vandenberghe and Nugteren, 2001; Moine *et al.*, 2017, 2021; Fischer *et al.*, 2020). However, the assumption that they correspond to waterlogged active layers has not been reconsidered.

LGM active layer thickness (ALT)

Assessment of ALTs, i.e. the thickness of the supra-permafrost layer that freezes in winter and thaws in summer, remains difficult to achieve from field data. According to Haesaerts and Van Vliet-Lanoë (1981), rapid vertical change in the microstructure created by segregation ice may help delineate the permafrost table, as sustained growth of ice lenses in the upper permafrost layer leads to strong soil compaction. However, the formation of an ice-rich transitional layer above the permafrost (Shur *et al.*, 2005; French and Shur, 2010) due to fluctuations in thawing depth on a decadal to centennial scale, and permafrost aggradation because of subsequent loess accumulation largely contribute to blurring the boundary. Periglacial involutions (cryoturbation), which develop in the active layer

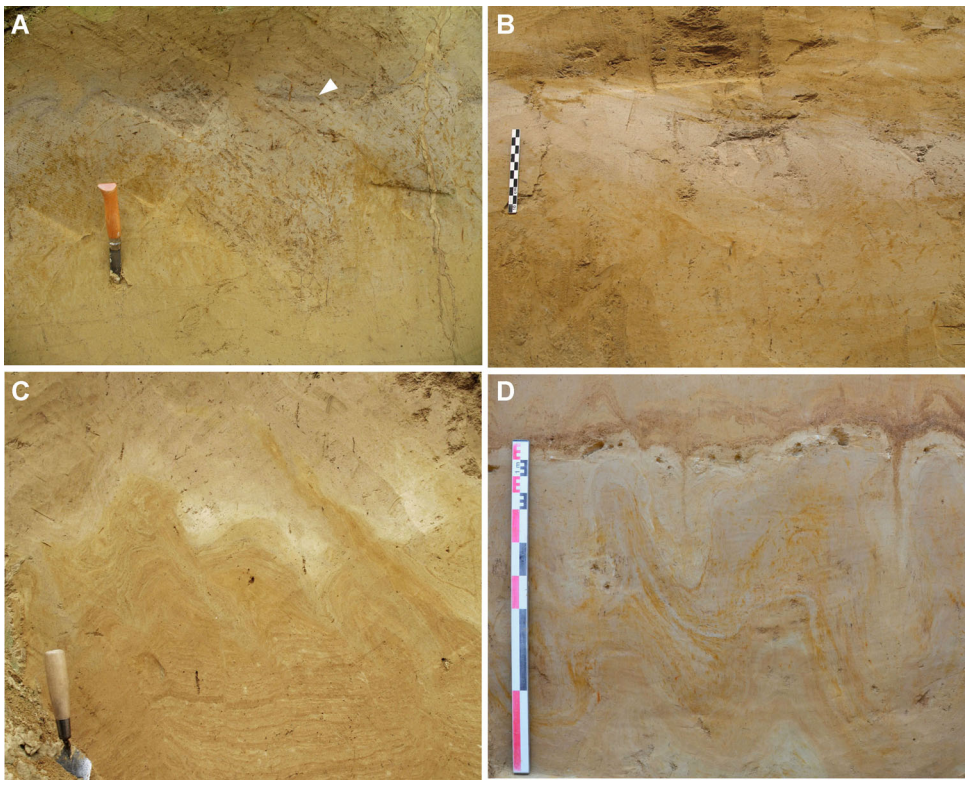

Figure 1. Views of 'tundra gleys' in loess sections. A, B, C – Kesselt (Belgium), D – Achenheim-Hischberg (France). In A, the bleached, dotted horizon overlies a thin brown Bw-like horizon. We can also distinguish an undulating, discontinuous grey brown (slightly organic) horizon a few millimetres thick at the top of the palaeosol (white arrow). Photo B illustrates the most common facies of 'tundra gleys', with a simple light grey horizon. The rule is 10 cm long. Photo C shows a bleached horizon overlying cryoturbated loess lacking clear evidence of gleying. The trowel is 23 cm long. In photo D, a bleached horizon overlies a thick gleyed cryoturbated horizon. The scale is 1 m long (photo P. Wuscher) [Color figure can be viewed at wileyonlinelibrary.com]

© 2022 The Authors. *Journal of Quaternary Science* Published by John Wiley & Sons Ltd.

in connection with freeze–thaw processes, may also provide some information on ALTs (e.g. Uxa *et al.*, 2021). In France, Bertran *et al.* (2017) showed that the depth of involution between 48° and 50°N (i.e. the latitude where ice-wedge pseudomorphs testify to the existence of permafrost) reaches up to 2 m and locally up to 2.5 m in coarse-grained alluvial deposits. Whether such a depth accurately reflects the ALT remains uncertain, however, as the involutions may have formed during permafrost degradation and active layer thickening (e.g. Murton *et al.*, 1995). Cryoturbation may also occur in areas affected by deep seasonal frost (i.e. without permafrost).

Therefore, palaeoclimate modelling is probably the best way to evaluate LGM ALTs in Europe. The outputs of the simulation (Fig. 2) allow us to draw the following conclusions:

(1) ALTs in the Northern European Loess Belt in France, Belgium and Germany were on average close to 2 m, and up to 3 m in some areas. Such values are consistent with those measured today in mineral soils in European high-altitude permafrost areas (Harris *et al.*, 2009; Rödder and Kneisel, 2012).
(2) In contrast to Stadelmaier *et al.* (2021), who considered only the −0.7 m ground level and failed to reconstruct permafrost where ALT was greater, the extent of permafrost based on the lowermost soil layer of the model with a representative depth of 1.5 m is in good agreement with the distribution of ice-wedge pseudomorphs documented by Isarin *et al.* (1998) and Andrieux *et al.* (2016).

Discussion

The genesis of 'tundra gleys'

Many arguments lead to the conclusion that most of the 'tundra gleys' cannot be waterlogged active layers. These are as follows:

(1) The bleached horizons have a low (3–30 cm) thickness, much less than expected for an active layer in mid-latitudes because of higher insolation than in modern Arctic regions. Accordingly, the regional WRF simulation shows that ALTs ranged between 2 and 3 m during the LGM in the Northern European Loess Belt where the 'tundra gleys' have been described. Episodes slightly colder than the LGM occurred between ca. 31 and 24 ka (referred to as the Last Permafrost Maximum; Vandenberghe *et al.*, 2014; Bertran *et al.*, 2014) and may have led to permafrost aggradation. However, ALTs lower than 0.5 m (and a fortiori lower than 0.3 m) are not realistic, as they would imply significant southward permafrost extension, which is contradictory to field evidence. Currently, ALTs lower than 0.5 m in mineral soils are only documented in the continuous permafrost area of the High Arctic and Antarctica. In the well-studied Mackenzie valley area (NWT, Canada, mean annual air temperature ca. −10 °C), the mean ALT in mineral soils, i.e. with a peat cover less than 15 cm, ranges between 55 and 108 cm (Smith *et al.*, 2009).
(2) The presence of earthworms producing calcite granules, which are currently absent in permafrost areas, and the molluscan assemblages are consistent with temperature improvement during the formation of these horizons, which is contradictory to the permafrost hypothesis. Radiocarbon ages on charcoals, molluscan shells and earthworm granules closely match those of interstadials (Vandenberghe and Nugteren, 2001; Moine *et al.*, 2017, 2021; Fischer *et al.*, 2020). Earthworms, which feed on organic material, suggest that vegetation developed at that time.
(3) In more continental Eastern Europe (Ukraine; e.g. Haesaerts *et al.*, 2003; Veres *et al.*, 2018), 'tundra gleys' become rarer in the LPS and are replaced by dark grey to black humic horizons of similar thickness and age. Transitional horizons between black humic and light grey, organic-poor horizons are frequent. In fact, high-resolution measurements in the Schwalbenberg LPS, Germany (Fischer *et al.*, 2020), clearly demonstrate organic matter (total organic carbon) enrichment in 'gelic gleysols' compared to loess. As mentioned above, 'tundra gleys' may also overlie a Bw-like horizon with a brighter colour (referred to as 'calcaric cambisol' in Fischer *et al.*, 2020), strongly suggesting that they are part

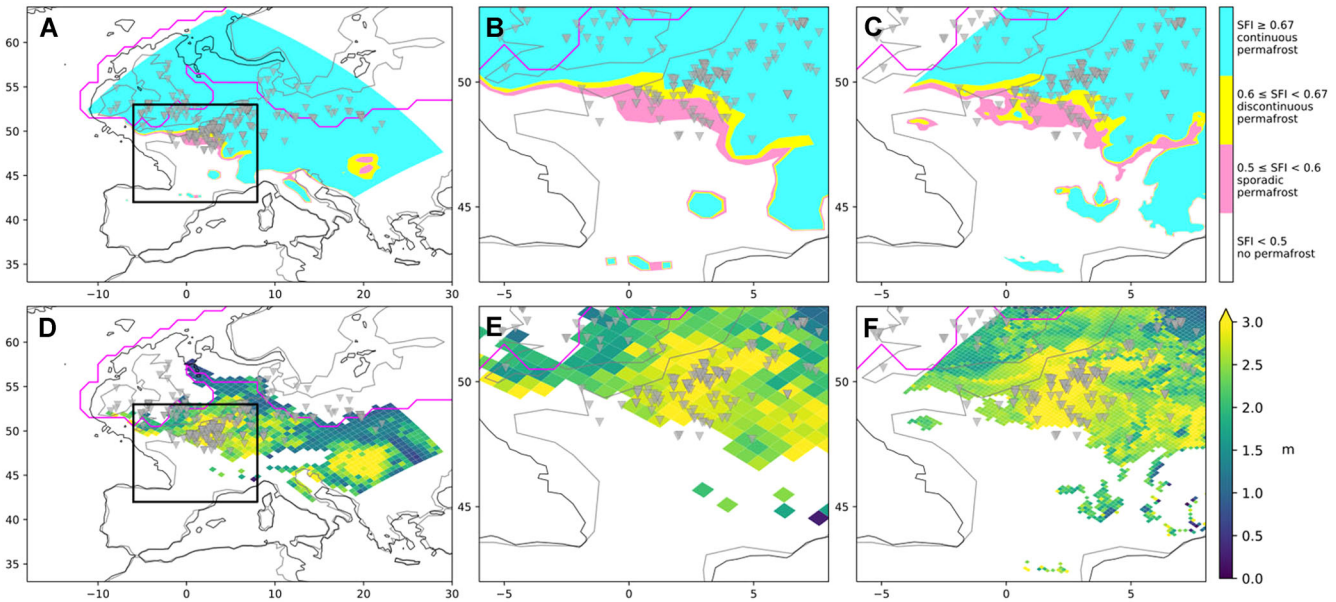

Figure 2. Permafrost (A–C) and ALT (D–F) distribution derived from the regional WRF simulation with 50-km horizontal resolution (A, B and D, E) and 12.5-km horizontal resolution (C, F). The solid rectangle marks the area of subfigures B, C and E, F. Thick black lines denote the LGM coastline, while pink lines denote the LGM ice sheet. Ice-wedge pseudomorphs from Andrieux *et al.* (2016) and Isarin *et al.* (1998) are highlighted with grey triangles [Color figure can be viewed at wileyonlinelibrary.com]

© 2022 The Authors. *Journal of Quaternary Science* Published by John Wiley & Sons Ltd.

(i.e. the topsoil horizon) of more complex soil profiles (Haesaerts and Van Vliet-Lanoë, 1981) (Fig. 1A).

(4) Similar horizons are found in regions that were never affected by permafrost, i.e. the lower Rhône valley, south-east France (Bosq *et al.*, 2020), and the Landes region, south-west France (Sitzia *et al.*, 2015) (Fig. 3). In the latter area, some examples clearly correspond to the loamy topsoil horizon of an incipient podzol developed on aeolian sand. The loamy texture indicates that the aeolian transport of sand-sized particles decreased, probably due to their capture by vegetation near the source areas, while inputs of finer-grained particles persisted.

All of this evidence argues against the assumption that all grey horizons represent former waterlogged active layers and, therefore, 'tundra gleys' as originally defined by Tedrow (1966). Rather, they correspond to organic-poor, bleached surface or subsurface horizons (Ag or Eg) buried under loess (or aeolian sand), which developed during climate ameliorations. As already suggested by Bosq *et al.* (2020), the poor content in organic matter (OM) may result from:

(1) Weak OM accumulation due to discontinuous, mostly herbaceous and/or cryptogamic (Smalley *et al.*, 2011; Svirčev *et al.*, 2019) vegetation cover and short periods of development. Available chronological data for late MIS 3 interstadials show that these lasted only a few centuries (Rasmussen *et al.*, 2014), which was not enough for large OM accumulation and maturation. Thin organic horizons may have been present in many cases, but have been not preserved because of subsequent erosion.

(2) OM degradation by soil microorganisms during burial. Unlike the humic horizons described in the LPS of Eastern Europe (e.g. Haesaerts *et al.*, 2003; Veres *et al.*, 2018), soil-forming conditions in less continental regions led to the formation of poorly condensed OM with low 'black carbon' content (Eckmeier *et al.*, 2007; Schmidt and Noack, 2000), which was less resistant to degradation. As vegetation was more shrubby during interstadials in Eastern Europe than in Western Europe (Svenning *et al.*, 2008; Magyari *et al.*, 2014) and, therefore, more prone to burning, the formation of highly resistant aromatic compounds was favoured in the east.

In a seminal paper written in French, Haesaerts and Van Vliet-Lanoë (1981) described in detail 'tundra gleys' at Harmignies, Belgium, and refined the interpretations they had proposed in an earlier paper (Haesaerts and Van Vliet-Lanoë, 1973). In particular, they rejected the hypothesis of a waterlogged active layer. The best-developed soil profile (units H.C.6–H.C.1, thermoluminescence- and infrared stimulated luminescence-dated to between 23 and 26 ka; Frechen *et al.*, 2001) comprises a suite of horizons, including an upper slightly organic grey brown horizon, grey horizons showing Fe–Mn precipitates and a lower yellow brown horizon. The greyish colour, which was restricted to the upper soil horizons, was assumed to reflect Fe depletion (responsible for the

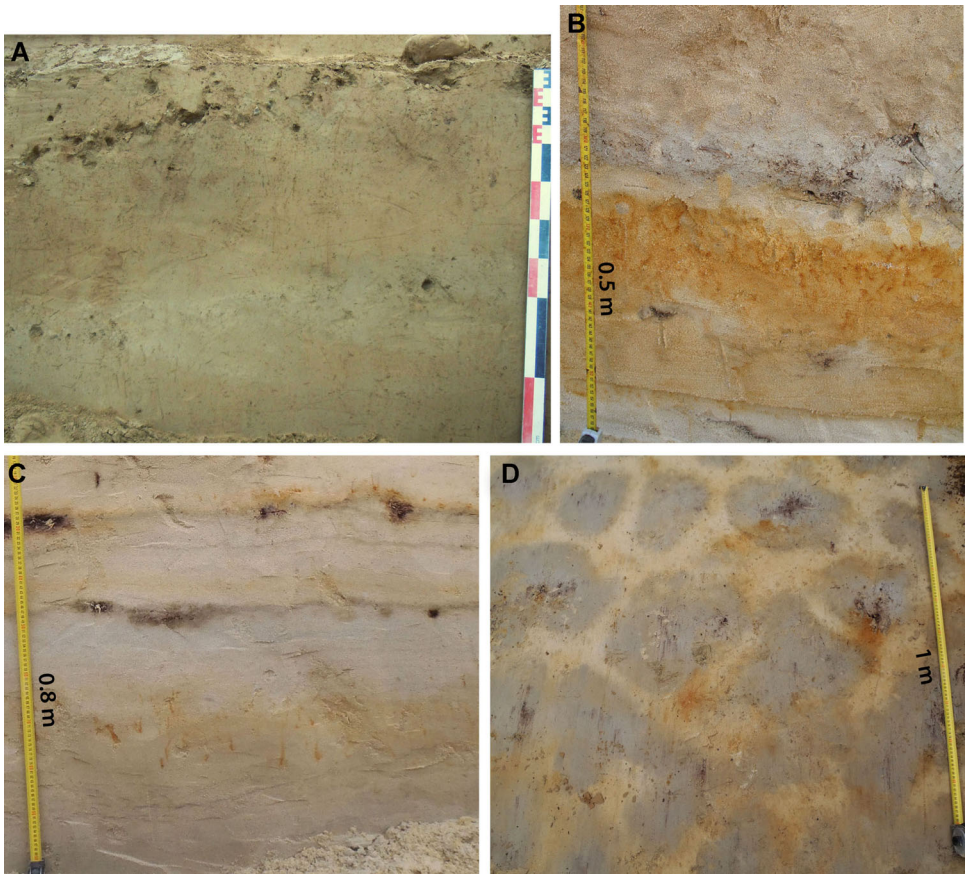

Figure 3. Views of Late MIS 3/MIS 2 organic-poor, Fe-depleted topsoil horizons from southern France. A – P2 palaeosol in the Lautagne loess section (44.9°N, south-east France) ^{14}C-dated to 27.7–27.3 ka cal BP, from Bosq *et al.* (2020); B – loamy topsoil Ag horizon overlying incipient E and Bs horizons on aeolian sand showing Fe oxide precipitates along former roots, Mont-de-Marsan (43.9°N, south-west France); C – incipient Ag–E–Bs profile on an aeolian sand ridge, Pontonx (43.8°N, south-west France), optically stimulated luminescence-dated to 23.4 ± 1.2 ka; the black spots correspond to local organic matter accumulation associated with modern roots; D – plan view of the Pontonx palaeosol in an inter-ridge depression showing a polygonal pattern due to frost action. According to Andrieux *et al.* (2016) and Stadelmaier *et al.* (2021), these sites were not affected by permafrost but were subject to deep seasonal frost [Color figure can be viewed at wileyonlinelibrary.com]

© 2022 The Authors. *Journal of Quaternary Science* Published by John Wiley & Sons Ltd.

persisting light colour despite the oxidizing conditions currently prevailing in the deposits) due to eluviation, possibly the formation of soluble Fe complexes with organic acids (i.e. podzolisation), and subsurface waterlogging below snow patches (Van Vliet-Lanoë, 1992). These processes (except for podzolisation in non-decalcified soils), together with OM degradation as outlined above, best explain the bleaching and oxide precipitation in the topsoil and subsurface horizons.

In their paper, Haesaerts and Van Vliet-Lanoë (1981) considered the presence of ice-wedge pseudomorphs below some (but not all) grey horizons to be a clear indication of their development in an active layer, whose thickness was assumed to reach ca. 80 cm, in better agreement with the expected ALT in this area. As outlined above, permafrost is contradictory to the evidence of climate amelioration in the topsoil horizon. Therefore, permafrost development and grey topsoil formation should be considered distinct, diachronic and unrelated events. As is usually the case in soil archives, disentangling the succession of pedological features remains difficult and the question of whether some features developed during the permafrost phase or later is difficult to resolve. Some LPS show that some bleached horizons developed during permafrost degradation and filled in part the ice-wedge pseudomorphs (Haesaerts and Van Vliet-Lanoë, 1981; Antoine *et al.*, 2014).

Main implications

Reinterpretation of most bleached horizons as weakly developed topsoil Ag or Eg horizons rather than waterlogged active layers has strong implications for their significance in the loess record, mainly:

(1) They formed during climate ameliorations associated with vegetation (cryptogams, herbs) development, possibly limited by long-lasting snow cover. Isolated Ag/Eg horizons probably developed during short (less than a century) climate ameliorations or a local decrease in loess deposition, whereas those associated with a more complete soil profile (i.e. with an underlying Bw horizon) correspond to longer interstadials.

(2) The recurrent formation of bleached horizons in some LPS (up to 12 during the Last Glacial in Nussloch, Germany; Antoine *et al.*, 2009) does not reflect repetitive events of permafrost development or permafrost accretion following sedimentation (syngenetic permafrost). In contrast, bleached horizons developed during periods of reduced or no sedimentation, which are not linked to permafrost. Therefore, without strong evidence such as ice-wedge pseudomorphs (which are scarce in the loess record), the identification of permafrost events should not rely on the occurrence of 'tundra gleys'. Palaeosols showing an upper bleached (Eg or A/Eg) horizon overlying a thick cryoturbated mottled Cg horizon may have formed in an active layer that later evolved under milder interstadial conditions (it should be kept in mind, however, that cryoturbation and solifluction can occur in areas without permafrost). Only a few palaeosols show such evidence. Figure 1D illustrates such a palaeosol from Achenheim-Hischberg, whose thickness reaches ca. 1 m.

(3) Earthworm granules show that bioturbation was active. Large granules [>0.5 mm in diameter, i.e. those used by Moine *et al.* (2021) for ^{14}C dating] were probably produced by the genus *Lumbricus* (Canti, 2007). Intense soil mixing due to the activity of anecic earthworms is a well-documented process (e.g. Johnson, 2002). Freeze–thaw processes (cryoturbation, solifluction) may also have favoured sediment mixing. Therefore, the assemblages of fossils found in these horizons probably provide a complex picture that incorporates both climate change-related faunal fluctuations and mixing.

This question has also implications for understanding human–environment relationships. The bleached horizons correspond to periods of vegetation development, capable of sustaining herds of large herbivores followed by predators (including humans). Although scarce in north-west Europe, most Upper Palaeolithic sites are located in such horizons (e.g. Łanczont *et al.*, 2015; Sprafke *et al.*, 2020; Moine *et al.*, 2021). In contrast, tundra gleys refer to a polar desert environment, which, therefore, have a very different meaning.

Overall, this points to the danger of using genetic terms to name palaeosols, such as 'tundra gley' or 'arctic brown soil', which may prove to be inadequate because of improved understanding of the context of their formation. Modern soil classifications use horizons as key elements (i.e. A organic topsoil horizon, E eluvial subsurface horizon, Bw cambic horizon, etc.). The key horizons can be present in soils in a variety of contexts and climatic zones. As many palaeosols are truncated or strongly modified by subsequent climate changes (see, e.g., Fédoroff and Goldberg, 1982 for a conceptual approach), well-preserved soil profiles corresponding to modal soils of a given climate area and parent-material lithology remain exceptional. Therefore, key horizon labels should be preferred in LPS studies.

Conclusion

There are many arguments against the hypothesis that all the bleached horizons with Fe–Mn oxide precipitations in European LPS reflect former waterlogged active layers. Regional climate simulations show that ALTs ranged between 2 and 3 m during the LGM in the Northern European Loess Belt, which is much greater than the thickness of the bleached horizons. Even if some permafrost aggradation occurred during the coldest episodes, ALTs lower than 0.5 m appear unrealistic. These horizons better correspond to Fe-depleted, slightly humic topsoil horizons or eluvial horizons and should be referred to as (incipient) Ag or Eg horizons instead of 'tundra gleys'. Palaeosols with a bleached horizon overlying a thick cryoturbated Cg horizon potentially corresponding to a waterlogged active layer do exist, however, but are probably rare in LPS. Overall, the use of key horizon nomenclature as defined in soil classifications should be preferred in loess studies over more genetic terms.

According to the new interpretation proposed, most bleached horizons formed during interstadials associated with a decrease in loess sedimentation and with vegetation development, which attracted large herbivores. The likelihood of strong biological and periglacial mixing of the topsoil makes it difficult to precisely reconstruct palaeoecological changes from fossil assemblages.

Acknowledgements. Kim H. Stadelmaier thanks the AXA Research Fund for support. And Patrick Ludwig is supported by the Helmholtz Climate Initiative REKLIM (regional climate change; https://www.reklim.de/en, last accessed: 16 February 2022). This work used resources of the Deutsches Klimarechenzentrum (DKRZ) granted by its Scientific Steering Committee (WLA) under project ID 965. P. Wuscher provided the photo from Achenheim-Hischberg. J. Vandenberghe and two anonymous reviewers are warmly thanked for their constructive remarks on the manuscript.

Abbreviations. ALT, active layer thickness; LGM, Last Glacial Maximum; LPS, loess–palaeosol sequence; MIS, Marine Isotope Stage.

© 2022 The Authors. *Journal of Quaternary Science* Published by John Wiley & Sons Ltd.

References

Andrieux E, Bertran P, Saito K. 2016. Spatial analysis of the French Pleistocene permafrost by a GIS database. *Permafrost and Periglacial Processes* **27**: 17–30.

Antoine P, Rousseau DD, Moine O, Kunesch S, Hatté C, Lang A, Tissoux H, Zöller L. 2009. Rapid and cyclic aeolian deposition during the Last Glacial in European loess: a high-resolution record from Nussloch, Germany. *Quaternary Science Reviews* **28**: 2955–2973.

Antoine P, Goval E, Jamet G, Coutard S, Moine O, Hérisson D, Auguste P, Guérin G, Lagroix F, Schmidt E, Robert V, Debenham N, Meszner S, Bahain JJ. 2014. Les séquences lœssiques pléistocène supérieur d'Havrincourt (Pas-de-Calais, France): stratigraphie, paléoenvironnements, géochronologie et occupations paléolithiques. *Quaternaire* **25**: 321–368.

Bertran P, Andrieux E, Antoine P, Deschodt L, Font M, Sicilia D. 2017. Pleistocene involutions and patterned ground in France: examples and analysis using a GIS database. *Permafrost and Periglacial Processes* **28**(4): 710–725.

Bertran P. 2022. Distribution and characteristics of Pleistocene ground thermal contraction polygons in Europe from satellite images. *Permafrost and Periglacial Processes*. https://doi.org/10.1002/ppp.2137

Bosq M, Kreutzer S, Bertran P, Degeai JP, Dugas P, Kadereit A, Lanos P, Moine O, Paffner N, Queffelec A, Sauer D. 2020. Chronostratigraphy of two Late Pleistocene loess-palaeosol sequences in the Rhône Valley (southeast France). *Quaternary Science Reviews* **245**: 106473.

Canti MG. 2007. Deposition and taphonomy of earthworm granules in relation to their interpretative potential in Quaternary stratigraphy. *Journal of Quaternary Science* **22**: 111–118.

Eckmeier E, Gerlach R, Gehrt E, Schmidt MW. 2007. Pedogenesis of chernozems in Central Europe—a review. *Geoderma* **139**: 288–299.

Fédoroff N, Goldberg P. 1982. Comparative micromorphology of two Late Pleistocene paleosols (in the Paris basin). *Catena* **9**: 227–251.

Fischer P, Jöris O, Fitzsimmons KE *et al*. 2020. Millennial-scale terrestrial ecosystem responses to Upper Pleistocene climatic changes: 4D-reconstruction of the Schwalbenberg Loess-Palaeosol- Sequence (Middle Rhine Valley, Germany). *Catena* **196**: 104913.

Food and Agricultural Organization (FAO). 1974. *FAO UNESCO Soil Map of the World*. Volume 1, Legend. UNESCO, Paris, 59.

Frechen M, Van Vliet-Lanoë B, van den Haute P. 2001. The Upper Pleistocene loess record at Harmignies/Belgium – High-resolution terrestrial archive of climate forcing. *Palaeogeography, Palaeoclimatology, Palaeoecology* **173**: 175–195.

French H, Shur Y. 2010. The principles of cryostratigraphy. *Earth Science Reviews* **101**: 190–206.

Gullentops F. 1954. Contributions à la chronologie du Pléistocène et des formes du relief en Belgique. *Mémoire de l'Institut de Géologie de l'Université de Louvain* **18**: 125–252.

Gullentops F 1981. About the climate of the last glaciation in NW-Europe. In *Quaternary Climatic Variations in a Milankovitch Perspective*, 2th of June 1981, Université Catholique de Louvain, Louvain, 1–5.

Haesaerts P, Van Vliet-Lanoë B. 1973. Evolution d'un permafrost fossile dans les limons du dernier glaciaire à Harmignies (Belgique). *Bulletin de l'Association Française pour l'Etude du Quaternaire* **10**(3): 151–164.

Haesaerts P, Van Vliet-Lanoë B. 1981. Phénomènes périglaciaires et sols fossiles observés à Maisières-Canal, à Harmignies et à Rocourt. *Biuletyn Peryglacjalny* **28**: 208–216.

Haesaerts P, Borziak I, Chirica V, Damblon F, Koulakovska L, van der Plicht J. 2003. The East Carpathian loess record: a reference for the Middle and Late Pleniglacial stratigraphy in Central Europe. *Quaternaire* **14**(3): 163–188.

Harris C, Arenson LU, Christiansen HH, Etzelmüller B, Frauenfelder R, Gruber S, Haeberli W, Hauck C, Hoelzle M, Humlum O, Isaksen K, Kääb A, Kern-Luetschg MA, Lehning M, Matsuoka N, Murton JB, Noetzli J, Phillips M, Ross N, Seppälä M, Springman S, Vonder Mühll D. 2009. Permafrost and climate in Europe: monitoring and modelling thermal, geomorphological and geotechnical responses. *Earth Science Reviews* **92**: 117–171.

Isarin R, Huijzer B, van Huissteden K. 1998. Time-slice oriented multiproxy database (MPDB) for palaeoclimatie reconstruction. National Snow and Ice Data Center, University of Boulder, Colorado. http://nsidc.org/data/ggd248.html

IUSS Working Group WRB. 2015. *World Reference Base for Soil Resources 2014, Update 2015: International Soil Classification System for Naming Soils and Creating Legends for Soil Maps*. Food and Agricultural Organization (FAO): Rome.

Johnson DL. 2002. Darwin would be proud: bioturbation, dynamic denudation, and the power of theory in science. *Geoarchaeology: An International Journal* **17**(1): 7–40.

Jungclaus JH, Fischer N, Haak H, Lohmann K, Marotzke J, Matei D, Mikolajewicz U, Notz D, von Storch JS. 2013. Characteristics of the ocean simulations in the Max Planck Institute Ocean Model (MPIOM) the ocean component of the MPI-Earth system model. *Journal of Advances in Modeling Earth Systems* **5**: 422–446. https://doi.org/10.1002/jame.20023

Kadereit A, Kind CJ, Wagner GA. 2013. The chronological position of the Lohne Soil in the Nussloch loess section - re-evaluation for a European loess-marker horizon. *Quaternary Science Reviews* **59**: 67–86.

Kitover DC, van Balen RT, Roche DM, Vandenberghe J, Renssen H. 2016. LGM Permafrost Thickness and Extent in the Northern Hemisphere derived from the Earth System Model iLOVECLIM. *Permafrost and Periglacial Processes* **27**: 31–42.

Koven CD, Riley WJ, Stern A. 2013. Analysis of Permafrost Thermal Dynamics and Response to Climate Change in the CMIP5 Earth System Models. *Journal of Climate* **26**(6): 1877–1900. https://doi.org/10.1175/JCLI-D-12-00228.1

Łanczont M, Madeyska T, Mroczek P, Komar M, Łącka B, Bogucki A, Sobczyk K, Wilczyński J. 2015. The loess-palaeosol sequence in the Upper Palaeolithic site at Krakow Spadzista: A palaeoenvironmental approach. *Quaternary International* **365**: 98–113.

Levavasseur G, Vrac M, Roche DM, Paillard D, Martin A, Vandenberghe J. 2011. Present and LGM permafrost from climate simulations: contribution of statistical downscaling. *Climate of the Past* **7**: 1647–1962.

Magyari EK, Kuneš P, Jakab G, Sümegi P, Pelánková B, Schäbitz F, Braun M, Chytrý M. 2014. Late Pleniglacial vegetation in eastern-central Europe: are there modern analogues in Siberia? *Quaternary Science Reviews* **95**: 60–79.

Moine O, Rousseau DD, Antoine P. 2008. The impact of Dansgaard–Oeschger cycles on the loessic environment and malacofauna of Nussloch (Germany) during the Upper Weichselian. *Quaternary Research* **70**: 91–104.

Moine O, Antoine P, Coutard S, Guérin G, Hatté C, Paris C, Saulnier-Copard S. 2021. Intra-interstadial environmental changes in Last Glacial loess revealed by molluscan assemblages from the Upper Palaeolithic site of Amiens-Renancourt 1 (Somme, France). *Journal of Quaternary Science* **36**(8): 1322–1340.

Murton JB, Whiteman CA, Allen P. 1995. Involutions in the Middle Pleistocene (Anglian) Barham Soil, eastern England: a comparison with thermokarst involutions from arctic Canada. *Boreas* **24**: 269–280.

Nelson FE, Outcalt SI. 1987. A Computational Method for Prediction and Regionalization of Permafrost. *Arctic and Alpine Research* **19**: 279–288. https://doi.org/10.1080/00040851.1987.12002602

Rasmussen SO, Bigler M, Blockley SP, Blunier T, Buchardt SL, Clausen HB, Cvijanovic I, Dahl-Jensen D, Johnsen SJ, Fischer H. 2014. A stratigraphic framework for abrupt climatic changes during the Last Glacial period based on three synchronized Greenland ice-core records: refining and extending the INTIMATE event stratigraphy. *Quaternary Science Reviews* **106**: 14–28.

Rödder T, Kneisel C. 2012. Influence of snow cover and grain size on the ground thermal regime in the discontinuous permafrost zone, Swiss Alps. *Geomorphology* **175-176**: 175–189.

Rohdenburg H, Meyer B. 1966. Zur Feinstratigraphie und Paläeopedologie des Jungpleistozäns nach Untersuchungen an Südniedersächsischen und Nordhessischen Lössprofilen. *Mitteilungen Deutche Bodenkundliche Gesellschaft* **5**: 1–170.

© 2022 The Authors. *Journal of Quaternary Science* Published by John Wiley & Sons Ltd.

Schmidt C, Zeeden C, Krauß L, Lehmkuhl F, Zöller L. 2021. A chronological and palaeoenvironmental re-evaluation of two loess-palaeosol records in the northern Harz foreland, Germany, based on innovative modelling tools. *Boreas* **50**: 746–763.

Schmidt MW, Noack AG. 2000. Black carbon in soils and sediments: analysis, distribution, implications, and current challenges. *Global Biogeochemical Cycles* **14**: 777–793.

Shur Y, Hinkel KM, Nelson FE. 2005. The Transient Layer: Implications for Geocryology and Climate-Change Science. *Permafrost and Periglacial Processes* **16**: 5–17.

Skamarock WC, Klemp JB, Dudhia J, Gill DO, Liu Z, Berner J, Wang W, Powers JG, Duda MG, Barker D, Huang XY, Wang W. 2019. *A Description of the Advanced Research WRF version 4*. National Center for Atmospheric Research, Technical Note NCAR/TN-566+STR, 145 pp. (https://doi.org/10.5065/1dfh-6p97)

Smith SL, Wolfe SA, Riseborough DW, Nixon FM. 2009. Active-Layer Characteristics and Summer Climatic Indices, Mackenzie Valley, Northwest Territories, Canada. *Permafrost and Periglacial Processes* **20**: 201–220.

Sitzia L, Bertran P, Bahain JJ, Bateman M, Hernandez M, Garon H, De Lafontaine G, Mercier N, Leroyer C, Queffelec A, Voinchet P. 2015. The quaternary coversands of southwest France. *Quaternary Science Reviews* **124**: 84–105.

Smalley I, Marković SB, Svirčev Z. 2011. Loess is [almost totally formed by] the accumulation of dust. *Quaternary International* **240**: 4–11.

Sprafke T, Schulte P, Meyer-Heintze S, Händel M, Einwögerer T, Simon U, Peticzka R, Schäfer C, Lehmkuhl F, Terhorst B. 2020. Paleoenvironments from robust loess stratigraphy using high-resolution color and grain-size data of the last glacial Krems-Wachtberg record (NE Austria). *Quaternary Science Reviews* **248**: 106602.

Stadelmaier KH, Ludwig P, Bertran P, Antoine P, Shi X, Lohmann G, Pinto JG. 2021. A new perspective of permafrost boundaries in France during the Last Glacial Maximum. *Climate of the Past* **17**: 2559–2576.

Stevens B, Giorgetta M, Esch M, Mauritsen T, Crueger T, Rast S, Salzmann M, Schmidt H, Bader J, Block K, Brokopf R, Fast I, Kinne S, Kornblueh L, Lohmann U, Pincus R, Reichler T, Roeckner E. 2013. Atmospheric component of the MPI-M Earth System Model: ECHAM6. *Journal of Advances in Modeling Earth Systems* **5**: 146–172. https://doi.org/10.1002/jame.20015

Svenning JC, Normand S, Kageyama M. 2008. Glacial refugia of temperate trees in Europe: insights from species distribution modelling. *Journal of Ecology* **96**: 1117–1127.

Svirčev Z, Dulić T, Obreht I, Codd GA, Lehmkuhl F, Marković S, Hambach U, Meriluoto J. 2019. Cyanobacteria and loess—an underestimated interaction. *Plant Soil* **439**: 293–308.

Tedrow J. 1966. Polar desert soils. *Soil Science Society of America Journal* **30**: 381–387.

Tedrow J. 1968. Pedogenic gradients in Polar Regions. *Journal of Soil Science* **19**(1): 197–204.

Terhorst B, Sedov S, Sprafke T, Peticzka R, Meyer-Heintze S, Kühn P, Solleiro Rebolledo E. 2015. Austrian MIS 3/2 loess-palaeosol records - Key sites along a west-east transect. *Palaeogeography, Palaeoclimatology, Palaeoecology* **418**: 45–56.

Tewari M, Chen F, Wang W, Dudhia J, LeMone MA, Mitchell K, Ek M, Gayno G, Wegiel J, Cuenca RH. 2004. Implementation and verification of the unified NOAH land surface model in the WRF model, in: 20th conference on weather analysis and forecasting/ 16th conference on numerical weather prediction, Seattle, WA, 10-16 January 2004, 11–15. (https://ams.confex.com/ams/84Annual/techprogram/paper_69061.htm, last access: 3 February 2022)

Uxa T, Křížek M, Hrbáček F. 2021. PERICLIMv1.0: a model deriving palaeo-air temperatures from thaw depth in past permafrost regions. *Geoscientific Model Development* **14**: 1865–1884.

Vandenberghe J, Nugteren G. 2001. Rapid climatic changes recorded in loess successions. *Global and Planetary Change* **28**(1/4): 1–9.

Vandenberghe J, Huijzer BS, Mücher H, Laan W. 1998. Short climatic oscillations in a western European loess sequence (Kesselt, Belgium). *Journal of Quaternary Science* **13**(5): 471–485.

Vandenberghe J, French H, Gorbunov A, Marchenko S, Velichko AA, Jin H, Cui Z, Zhang T, Wan X. 2014. The Last permafrost Maximum (LPM) map of the Northern Hemisphere: permafrost extent and mean annual air temperatures, 25-17 ka. *Boreas* **43**: 652–666.

Van Vliet-Lanoë B. 1992. Le niveau à langues de Kesselt, horizon repère de la stratigraphie du Weichsélien supérieur européen: signification paléoenvironnementale et paléoclimatique. *Bulletin de la Société Géologique de France* **160**: 35–44.

Veres D, Tecsa V, Gerasimenko N, Zeeden C, Hambach U, Timar-Gabor A. 2018. Short-term soil formation events in last glacial east European loess, evidence from multi-method luminescence dating. *Quaternary Science Reviews* **200**: 34–51.

© 2022 The Authors. *Journal of Quaternary Science* Published by John Wiley & Sons Ltd.